Defense Technical Information Center Compilation Part Notice

ADP012665

TITLE: Oxidation Kinetics and Microstructure of Wet-Oxidized MBF-Grown Short-Period AlGaAs Superlattices

DISTRIBUTION: Approved for public release, distribution unlimited

This paper is part of the following report:

TITLE: Progress in Semiconductor Materials for Optoelectronic Applications Symposium held in Boston, Massachusetts on November 26-29, 2001.

To order the complete compilation report, use: ADA405047

The following component part numbers comprise the compilation report:
ADP012585 thru ADP012685

Mat. Res. Soc. Symp. Proc. Vol. 692 © 2002 Materials Research Society H9.44

Oxidation Kinetics and Microstructure of Wet-Oxidized MBE-Grown Short-Period AlGaAs Superlattices

René Todt[1], Katharine Dovidenko, Alexei Katsnelson, Vadim Tokranov, Michael Yakimov, and Serge Oktyabrsky
UAlbany Institute for Materials, University at Albany-SUNY,
Albany, NY 12203, U.S.A.
[1] currently Walter Schottky Institute, Technical University Munich,
85748 Garching, Germany

ABSTRACT

The kinetics of the wet oxidation process of MBE-grown high-Al-content AlAs/$Al_{0.6}Ga_{0.4}As$ short-period superlattices (SPSLs) was investigated and compared to AlGaAs alloys and pure AlAs. We found that alloys and superlattices (SLs) have different oxidation characteristics. These differences were attributed to traces of the superlattice structure in the oxidized material. The microstructure and chemistry of SPSLs with an equivalent composition of $Al_{0.98}Ga_{0.02}As$ was studied, using transmission electron microscopy, energy-dispersive x-ray spectroscopy, Rutherford backscattering, and nuclear reaction analysis for hydrogen-profiling. We also report on the mechanical stability of oxidized SPSL layers in optoelectronic device structures.

INTRODUCTION

Recently, selective wet oxidation of AlGaAs alloys has gained interest for various applications in electronic and optoelectronic devices [1-3]. So far, wet oxidation has had its biggest impact on performance of AlGaAs/GaAs oxide-apertured vertical cavity surface emitting lasers (VCSELs), where devices with the lowest threshold currents and highest wall plug efficiency have been demonstrated [4]. As it is well known by now that VCSELs employing oxidized AlAs layers suffer from delamination and degradation problems [5], high-Al-content AlGaAs layers are generally preferred as wet oxidation layers. Devices employing AlGaAs alloys as wet oxidation layer were reported to be mechanically stable [5]. Also, VCSEL devices with an AlAs/GaAs superlattice (SL) oxidation layer with an equivalent Al content of 98 % were reported to be mechanically stable during post-growth processing, except for minor structural degradations on the edge of the mesa [6].

Due to the high selectivity of the wet oxidation process with respect to the Al content of the layer to be oxidized, a precise control over the composition during molecular beam epitaxy (MBE) growth of the structure is required in order to achieve reproducible oxidations [7]. The growth of high-Al-content alloys is, however, problematic with respect to reproducibility. Short-period superlattices (SPSLs), also termed digital-alloys, provide an enhanced control over the composition as compared to alloys. In addition, digital alloys of a wide variety of compositions can be grown without changing the effusion cell temperatures. Moreover, SPSLs are of great technological importance in MBE growth of optoelectronic device structures as they grow more smoothly than alloys, which is especially important when very thick structures like VCSELs with a total thickness in excess of 10 µm are grown.

This paper reports on wet oxidation kinetics, structure chemistry and mechanical stability of $Al_xGa_{1-x}As$ SPSLs (x= 0.90-0.98), which are compared to $Al_xGa_{1-x}As$ alloys.

EXPERIMENTAL DETAILS

The structure used for the study of the oxidation kinetics was grown by MBE on GaAs(100) substrates. The high-Al-content layers used for oxidation were 1000 Å-thick and were separated by 1000 Å $Al_{0.1}Ga_{0.9}As$ layers. The high-Al-content $Al_xGa_{1-x}As$ layers were grown as SPSLs with equivalent Al concentrations of x = 0.90, 0.92, ..., 0.98, or as alloys with x = 0.96, 0.98. The SPSLs were grown as periodic (3-19 ML AlAs)/(1 ML $Al_{0.6}Ga_{0.4}As$) structures with a fixed 1 monolayer thickness of the $Al_{0.6}Ga_{0.4}As$ layers.

Post growth processing started with the definition of 300 µm wide stripe mesas by standard photolithography and chemical wet etching using a solution of $HCl:H_2O_2:H_2O$ (20:1:1). Oxidations were carried out at temperatures of 350, 400 and 450 °C for 30 to 120 min in a flow of wet nitrogen at atmospheric pressure. Wet nitrogen was produced by flowing dry nitrogen at a flow rate of 2.0 slm through a bubbler filled with deionized water, which was maintained at a temperature of 93 °C. After the oxidation, the samples were cleaved and the oxidation lengths were measured using cross-sectional scanning electron microscopy (SEM).

A sample for the study of the microstructure and composition of oxidized SPSLs with an equivalent Al content of 98 % consisted of 1686 Å $Al_{0.98}Ga_{0.02}As$ layers (1ML/29MLs of $Al_{0.4}Ga_{0.6}As$/AlAs) separated by 744 Å $Al_{0.4}Ga_{0.6}As$ layers. Immediately before wet oxidation, 60 µm wide stripe mesas were etched, and oxidation was carried out at 400 °C for 90 min.

RESULTS AND DISCUSSION

Oxidation kinetics

A cross-sectional SEM image of an oxidized structure, which was used for the measurement of the oxidation lengths, is shown in Figure 1. From the measurement of the oxidation lengths as a function of oxidation time, the oxide growth was observed to proceed linearly with time and the oxidation rates were determined as plotted in Figure 2. The oxidation rates decrease with decreasing Al-content, as expected, and one can observe that the oxidation rates of SLs are significantly higher than those of alloys with the equal average Al content. This difference in the oxidation rates between SLs and alloys is decreasing with increasing oxidation temperature and they become equal within the error of the experiment at 450 °C. This observation is in agreement with a report by Pickrell et al. who observed the same trend for an AlAs/GaAs SL with an effective Al content of 98 % [6]. Using a similar model as the one developed by Deal and Grove for the oxidation of silicon [8], the linear growing oxidation length x can be described in terms of an activation energy E_A as

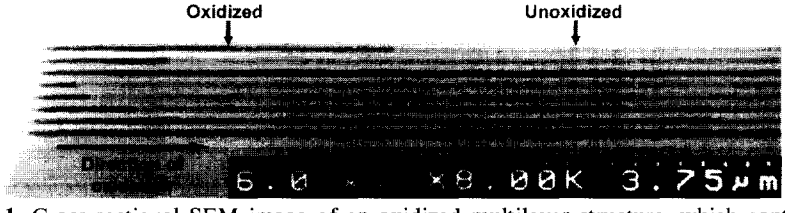

Figure 1. Cross-sectional SEM image of an oxidized multilayer structure, which contains several high-Al-content $Al_xGa_{1-x}As$ layers. From top to bottom: x = 0.98, 0.96 alloys, pure AlAs, x = 0.90, 0.92, ..., 0.98 SPSLs. The oxidation has been carried out at 400 °C.

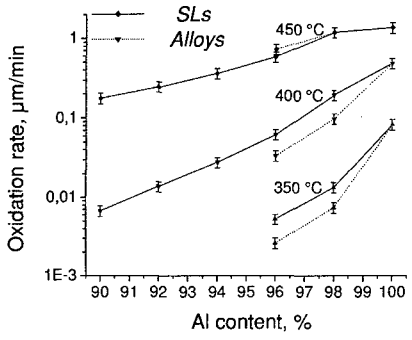

Figure 2. Oxidation rate vs. Al content.

$$x(t,T) = C\, t \exp\left(-\frac{E_A}{k_B T}\right), \qquad (1)$$

where C is a constant. Hence, an Arrhenius plot (Figure 3) of the oxidation rate (x/t) versus the inverse of the oxidation temperature T allows to determine E_A and C (Table I). The activation energies increase with decreasing Al content and the oxidation process of a SL has a lower activation energy than that of an alloy with the equal Al content. The determined activation energies for the alloys are in good agreement with literature values [9]. Our results clearly indicate that the oxidation processes of alloys and SPSLs are not identical.

Microstructure and composition of wet-oxidized AlGaAs short-period superlattices

To gain a more thorough understanding of the wet oxidation process of SPSLs, we investigated the microstructure of an $Al_{0.98}Ga_{0.02}As$ SPSL. Figure 4 shows a cross-sectional transmission electron microscope (TEM) image of the oxidized AlGaAs SL and its interface to an adjacent unoxidized $Al_{0.4}Ga_{0.6}As$ layer. The interface (indicated by arrows in Figure 4) between the oxidized and the adjacent unoxidized layer was observed to be rough. The image also clearly shows traces of the SL structure in the oxidized layer. Certainly, the presence of an ordered structure is a significant difference between oxidized SPSLs and alloys, which can explain for the different oxidation characteristics of alloys and SLs with the equal Al content.

The wet oxidized layers are quite porous, and the reaction kinetics is usually determined by the diffusion of the reactants through the dense

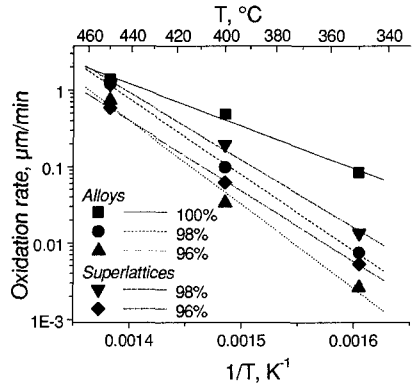

Figure 3. Arrhenius plot of the oxidation rate vs. the inverse oxidation temperature, illustrating the different temperature dependences of the wet oxidation process of SLs and alloys with the equal Al content.

Table I. Activation energies E_A and constants C as determined from an Arrhenius plot of the oxidation rates vs. the inverse temperature.

Al content	E_A, eV	C, µm/min
100 %	1.09 ± 0.11	18.0 ± 1.9
98 % alloy	1.97 ± 0.07	31.8 ± 1.1
96 % alloy	2.17 ± 0.06	34.5 ± 1.0
98 % SL	1.75 ± 0.02	28.3 ± 0.4
96 % SL	1.83 ± 0.12	28.8 ± 1.9

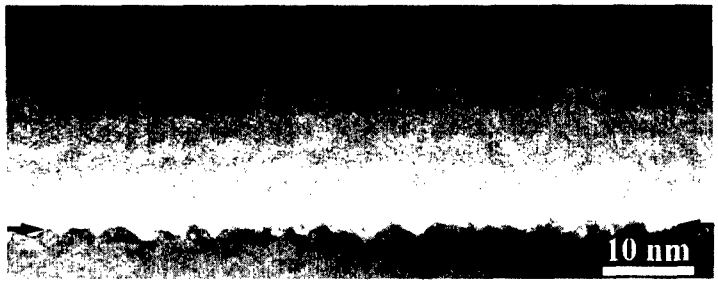

Figure 4. Cross-sectional bright field TEM image showing an oxidized $Al_{0.98}Ga_{0.02}As$ SPSL (upper part) and its interface (indicated by arrows) to an adjacent unoxidized $Al_{0.4}Ga_{0.6}As$ layer (lower part). Traces of the SL structure are clearly observed in the oxidized layer.

oxidation front. The properties of this oxidation front are very sensitive to the Ga content. Therefore, the presence of an ordered structure, such as the traces of the SL, provides an efficient path for diffusion of reactants (through areas without Ga) and results in an increased concentration of the oxidizing agent water at the reaction front. Hence, the oxidation rate is increased (assuming that the oxidation process is not reaction rate limited), which is in agreement with our observations at 350 and 400 °C. With increasing temperature, the diffusion through the dense oxidation front becomes faster and thus, the kinetics of the oxidation process is determined by the rate of reaction at the reaction front. Therefore, the difference in the oxidation rate of alloys and SLs with the equal Al contents will become smaller with increasing temperature until the oxidation rates of SLs and alloys finally become equal, which is also supported by our experimental results.

The oxidized $Al_{0.98}Ga_{0.02}As$ SLs have been observed to be unstable under electron beam exposure in the TEM, showing recrystallization and grain growth. This is in agreement with an earlier report in literature on the microstructure of wet oxidized AlGaAs alloys [10]. Selected area electron diffraction patterns (SADPs) taken during the observation in the TEM illustrate this crystallization process (Figure 5). At the very beginning of the observation, the SADP (Figure 5a) shows a diffuse pattern indicating an amorphous material. After several minutes of the electron beam exposure, a sharp ring pattern is formed (Figure 5b), corresponding to non-stoichiometric polycrystalline cubic γ-Al_2O_3 phase with a lattice constant of 7.9 Å (PDF file #74-2206).

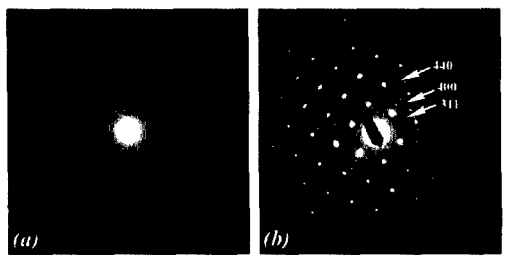

Figure 5. Selected area electron diffraction patterns from the oxidized SL showing crystallization under the electron beam. (a) At the beginning of the observation, showing an amorphous structure. (b) After several minutes of observation, showing a polycrystalline structure of cubic γ-Al_2O_3 phase.

Further investigations on the composition were carried out using energy dispersive x-ray spectroscopy (EDXS) and Rutherford backscattering (RBS). The results showed that As is evaporated upon wet oxidation and that only significant amounts of Al and O are present in the oxidized material, as was expected from

previous reports on the composition of oxidized AlGaAs alloys [10]. The composition of the oxidized $Al_{0.98}Ga_{0.02}As$ SL matches with an α-Al_2O_3 (sapphire) standard sample within 5 %.

Also the formation of aluminum hydroxides can be expected upon wet oxidation. Nuclear reaction analysis (NRA) was employed for hydrogen profiling in the oxidized $Al_{0.98}Ga_{0.02}As$ SPSL. NRA for hydrogen was carried out using a resonant nuclear reaction of ^{15}N and ^{1}H at a resonance energy of 6.385 MeV:

$$^{15}N + {}^{1}H \rightarrow {}^{12}C + {}^{4}He + \text{gamma-ray}. \quad (2)$$

A hydrogen depth profile was first measured for the as-oxidized sample. Subsequently, this sample was annealed at 450 °C in vacuum (~ 10^{-3} mbar) for 10 min and a second hydrogen depth profile was measured. Figure 6 shows the measured hydrogen depth profiles. In the as-oxidized sample, the hydrogen concentration in the oxidized layer was determined to be about 2 x 10^{22} cm^{-3}, which corresponds to an Al-to-H ratio of about 1:0.7. After annealing in vacuum, the hydrogen concentration is reduced significantly, and the determined Al-to-H ratio is about 1:0.2. High H concentration in the as-oxidized sample is likely due to absorption of water in the porous oxide layer, though the formation of aluminum hydroxides cannot be completely ruled out. After the vacuum anneal, most of the absorbed water is evaporated, and the hydrogen concentration is determined by the chemically bound H, presumably in the form of aluminum hydroxides.

Mechanical stability of oxide-apertured VCSELs and LEDs

We used $Al_{0.96}Ga_{0.04}As$ SPSL wet oxidation layers for the fabrication of oxide-apertured AlGaAs-based VCSELs. These devices had diameters ranging from 10 to 35 µm and were oxidized at 400 °C. Oxidation lengths were varied between 4 and 10 µm. We did not observe any structural degradation of these device structures upon wet oxidation or further processing.

For the fabrication of AlGaAs-based surface-emitting LEDs, oxidation lengths in excess of 10 µm were required. We employed a 1000 Å $Al_{0.98}Ga_{0.02}As$ SPSL, which was embedded in 2 µm thick $Al_{0.1}Ga_{0.9}As$ layers, as a wet oxidation layer. Upon wet oxidation, formation of cracks was observed. These cracks originated from the wet oxidation layer and propagated towards the top of the structure (Figure 7). Also a cavity can be observed to form at the origin point of the crack. Interestingly enough, the position of the cracks were found to be independent of the oxidation length for a particular structure. For the LED structure shown in the Figure 7, the cracks always originated at 20 µm from the mesa edge, indicating the existence of a critical stress and, therefore, a critical oxidation length. Cracking occurs due to the buildup of stress caused by the shrinkage of the high-Al-concentration layer upon wet oxidation. Such structural degradations were so far known only for pure AlAs oxidation layers. We envision that the critical oxidation length is a function of the composition of the

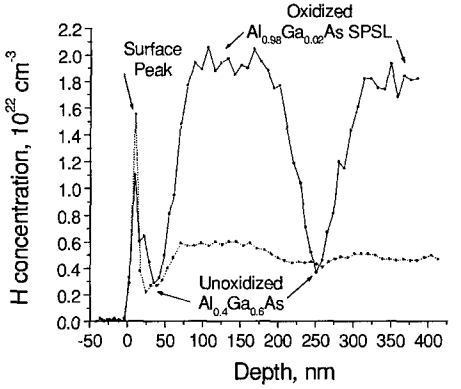

Figure 6. Hydrogen depth profiles of an as-oxidized sample (solid line) and of the same sample after annealing in vacuum (dotted line). The hydrogen concentration is strongly reduced after annealing of the sample in vacuum.

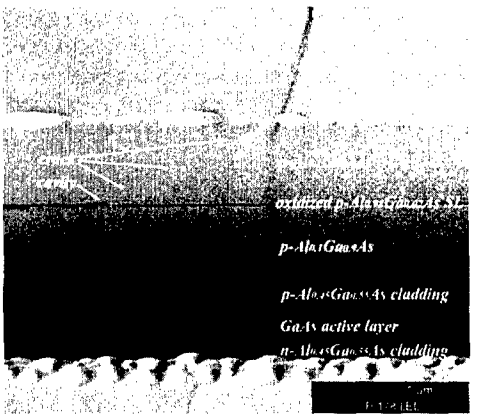

Figure 7. Focused ion beam (FIB) microscope image of the cross section of a LED structure oxidized through 40 μm. A crack (indicated by arrows) was formed upon wet oxidation and is originating from the oxidized AlGaAs SL to the surface of the structure.

oxidation layer as well as of the geometry and mechanical properties of the whole structure. Further efforts should be applied to establish the window for the mechanically stable oxidized structures.

CONCLUSIONS

In conclusion, we characterized the kinetics of the lateral wet oxidation process of high-Al-content short-period superlattices (SPSLs), investigated the microstructure and composition of an oxidized $Al_{0.98}Ga_{0.02}As$ SPSL, and reported on the mechanical stability of VCSELs and LEDs with an AlGaAs SPSL oxide aperture. The differences in the oxidation kinetics of SLs and alloys were explained by the presence of traces of the SL structure in the oxidized SPSL layer, which results in a higher oxidation rate of the SPSLs. The oxidized layer was found to have amorphous structure, and was recrystallized under the electron beam exposure during TEM observation to form a polycrystalline non-stoichiometric γ-Al_2O_3 phase. High hydrogen concentration (Al-to-H ratio of 1:0.7) was measured for an as-oxidized film, and we demonstrated that the hydrogen concentration was greatly reduced (3.5 times) by thermal annealing of the sample in vacuum. A critical oxidation length for the formation of cracks was observed for short-period superlattices with the equivalent composition of $Al_{0.98}Ga_{0.02}As$. Once this critical oxidation length is exceeded, cracks are formed, indicating the relaxation of the buildup stress.

ACKNOWLEDGMENT

This work has been supported by the National Focus Center for Interconnects for Gigascale Integration, funded by MARCO and DARPA.

REFERENCES

1. E. I. Chen, N. Holonyak, Jr., and S. A. Maranowski, Appl. Phys. Lett., **66**, 2688 (1995).
2. F. A. Kish, S. J. Caracci, et al., Appl. Phys. Lett., **59**, 1755 (1991).
3. D. L. Huffaker, D. G. Deppe, et al., Appl. Phys. Lett., **65**, 97 (1994).
4. L. A. Coldren, E. Hegblom, et al., SPIE Proc., **3003**, 2 (1997).
5. K. D. Choquette, K. M. Geib, et al., Appl. Phys. Lett., **69**, 1385 (1996).
6. G. W. Pickrell, J. H. Epple, et al., Appl. Phys. Lett., **76**, 2544 (2000).
7. J. M. Dallesasse, N. Holonyak, Jr., et al., Appl. Phys. Lett., **57**, 2844 (1990).
8. B. E. Deal, and A. S. Grove, J. Appl. Phys., **36**, 3770 (1965).
9. K. M. Geib, K. D. Choquette, et al., SPIE Proc., **3003**, 69 (1997).
10. R. D. Twesten, D. M. Follstaedt, and K. D. Choquette, SPIE Proc., **3003**, 55 (1997)